Evaluation of hemodynamic imaging findings of hypervascular hepatocellular carcinoma: Comparison between dynamic contrast-enhanced magnetic resonance imaging using radial volumetric imaging breath-hold examination with k-space-weighted image contrast reconstruction and dynamic computed tomography during hepatic arteriography

Masahiro Kurozumi,[1] Yasunari Fujinaga,[1*] Yoshihiro Kitou,[2] Akira Yamada,[1] Ayumi Ohya,[1] Yasuo Adachi,[2] Yoshinori Tsukahara,[1] Marcel D Nickel,[3] Katsuya Maruyama,[4] Takeshi Uehara,[5] Shin-ichi Miyagawa,[6] Masumi Kadoya[2]

[1]Department of Radiology, Shinshu University School of Medicine, 3-1-1 Asahi, Matsumoto 390-8621, Japan

[2]Radiology Division of Shinshu University Hospital, 3-1-1 Asahi, Matsumoto 390-8621, Japan

[3]Siemens Healthcare GmbH, Erlangen, Germany

[4]DI Research & Collaboration Dpt., Siemens Healthcare K.K., Shinagawa, Tokyo,

Japan

[5]Department of Laboratory Medicine, Shinshu University School of Medicine, 3-1-1 Asahi, Matsumoto 390-8621, Japan

[6]First Department of Surgery, Shinshu University School of Medicine, 3-1-1 Asahi, Matsumoto 390-8621, Japan

*Corresponding author/reprint requests: Yasunari Fujinaga, MD, PhD

Department of Radiology, Shinshu University School of Medicine

3-1-1 Asahi, Matsumoto 390-8621, Japan

Tel: +81-263-37-2650, Fax: +81-263-37-3087

E-mail: fujinaga@shinshu-u.ac.jp

Conflict of interest

The authors of this manuscript declare the relationships with the following companies:

Dr. Marcel Dominik Nickel is an employer of Siemens Healthcare GmbH, and Mr. Katsuya Maruyama is an employer of Siemens Healthcare K. K. The authors thank

these companies for allowing the use of the prototypical r-VIBE-KWIC for our study.

The other authors declare that they have no conflict of interest.

Type of manuscript: Original article

Abstract

Purpose

To compare the visualization of hemodynamic imaging findings of hypervascular hepatocellular carcinoma (HCC) on dynamic contrast-enhanced magnetic resonance imaging (DCE-MRI) using radial volumetric imaging breath-hold examination with k-space-weighted image contrast reconstruction (r-VIBE-KWIC) versus dynamic computed tomography during hepatic arteriography (dyn-CTHA).

Materials and Methods

We retrospectively reviewed the databases of preoperative DCE-MRI using r-VIBE-KWIC, dyn-CTHA, and postoperative pathology of resected specimens. Fourteen patients with 14 hypervascular HCCs underwent both DCE-MRI and dyn-CTHA. The imaging findings of the tumor and adjacent liver parenchyma were assessed on both modalities by two readers. The tumor enhancement time was also compared between the two modalities.

Results

On DCE-MRI/dyn-CTHA, early staining, peri-tumoral low-intensity or low-density

bands, corona enhancement, and washout of HCC were observed in 14/14 (100%), 10/12 (83%), 11/14 (78%), and 4/14 (29%) patients, respectively. Pathologically, four HCCs with low-density bands on dyn-CTHA had no fibrous capsules. The median tumor enhancement time on DCE-MRI and dyn-CTHA was 24 (9–24) and 23 (8–35) s, respectively. The correlation coefficient between the two groups was 0.762 ($P < 0.002$).

Conclusions

DCE-MRI using r-VIBE-KWIC has diagnostic potential comparable with that of dyn-CTHA in the hemodynamic evaluation of hypervascular HCC except for the washout phenomenon.

Keywords

dynamic contrast-enhanced magnetic resonance imaging; radial volumetric imaging breath-hold examination (VIBE) with k-space-weighted image contrast reconstruction; dynamic computed tomography during hepatic arteriography; hepatocellular carcinoma

Abbreviations

HCC	hepatocellular carcinoma
DCE-MRI	dynamic contrast-enhanced magnetic resonance imaging
VIBE	volumetric imaging breath-hold examination
KWIC	k-space-weighted image contrast reconstruction
dyn-CTHA	dynamic computed tomography during hepatic arteriography

Introduction

Evaluation of the arterial blood flow of the nodules is extremely useful in differentiation between advanced hepatocellular carcinoma (HCC) from early HCC and dysplastic nodules [1, 2], and it is important to determine the most appropriate therapeutic strategy [3]. The hemodynamic characteristics of HCC have been radiologically analyzed using various diagnostic imaging techniques such as dynamic contrast-enhanced computed tomography (CT) and CT during hepatic arteriography (CTHA). Single-level dynamic CTHA (dyn-CTHA) features high spatial and temporal resolution and is able to demonstrate the hemodynamic characteristics of HCC such as arterial hypervascularity, corona enhancement of the surrounding liver, and the washout phenomenon of arterial staining; it has historically been considered the gold standard method for hemodynamic analysis of HCC [4, 5]. However, CTHA is a critically invasive technique with the drawback of radiation exposure. Dynamic contrast-enhanced CT is less invasive than CTHA but also involves radiation exposure.

In contrast, magnetic resonance imaging (MRI) is less invasive and involves no radiation exposure. Dynamic contrast-enhanced MRI (DCE-MRI) is available for

dynamic study of the hemodynamics of HCC. Gadolinium ethoxybenzyl diethylenetriamine pentaacetic acid (Gd-EOB-DTPA), a hepatocyte-specific contrast agent, has been used worldwide for DCE-MRI of the liver. However, the volume used is half that of a nonspecific extracellular contrast agent; therefore, the adequate duration of acquisition is narrow, and it is difficult to obtain an optimal arterial phase. New three-dimensional gradient-echo sequences in MRI with high spatial and temporal resolution were recently developed and have been clinically applied. One of these techniques is the radial volumetric imaging breath-hold examination (r-VIBE), which is a modified version of Cartesian (traditional) VIBE (c-VIBE). The r-VIBE sequence offers several advantages over the c-VIBE sequence, including less motion sensitivity, the absence of aliasing artifact, and less degradation of the image quality due to undersampling [6, 7]. Furthermore, r-VIBE with k-space-weighted image contrast reconstruction (r-VIBE-KWIC) allows for powerful view-sharing and provides high-temporal-resolution sub-frame (time-resolved) images as well as a full-frame image, and optimal arterial images can be obtained in over 90% [8]. Therefore, without an invasive procedure or radiation exposure, DCE-MRI using r-VIBE-KWIC has the

potential to provide images with high temporal and spatial resolution that are as useful as dyn-CTHA for both detection and characterization of hypervascular hepatic lesions.

We compared the visualization of hemodynamic imaging findings of hypervascular HCC on DCE-MRI using r-VIBE-KWIC versus dyn-CTHA.

Materials and Methods

This study was approved by the institutional review board of our hospital, and written informed consent was obtained from all of the enrolled patients.

Patients

We retrospectively reviewed the DCE-MRI, dyn-CTHA, and pathology databases in our institution. From March 2012 to November 2012, 36 consecutive patients whose liver nodules had been wholly resected and histologically diagnosed as HCC were enrolled in this study. Of the 36 patients, 3 did not undergo DCE-MRI using r-VIBE-KWIC, 13 did not undergo dyn-CTHA, and 4 did not undergo either examination. One patient had a huge tumor and portal vein thrombus, and one patient had a hypovascular HCC on

dynamic contrast-enhanced CT. These 22 patients were excluded from this study because their conditions were determined inappropriate for the study concept. Finally, the remaining 14 patients (9 men, 5 women; mean age, 67.9 years) with 14 HCCs (mean diameter, 20.3 mm; range, 13–31 mm) who had undergone both DCE-MRI using r-VIBE-KWIC and dyn-CTHA before surgery were selected for this study. Three patients were infected with hepatitis B virus, eight with hepatitis C virus, and two with both hepatitis B and C virus; one patient had alcoholic liver disease. Liver function was evaluated with the Child–Pugh classification system; all patients had class A liver function.

DCE-MRI

All MR images were obtained with a 3T MRI unit (MAGNETOM Trio; Siemens Healthcare, Erlangen, Germany) using a standard body array coil with six channels and a spine matrix coil with six channels provided by the manufacturer. The scan parameters of DCE-MRI using r-VIBE-KWIC are shown in Table 1.

The arterial phase of DCE-MRI was performed using r-VIBE-KWIC reconstruction

(eight sub-frames; temporal resolution, 2.6–3.0 s) 25 s after the beginning of venous injection of Gd-EOB-DTPA (injection rate, 2 mL/s), followed by the portal venous phase (45 s after arterial phase; full-frame images; temporal resolution, 21–24 s) and late phase (90 s after arterial phase; full-frame images; temporal resolution, 21–24 s) (Fig. 1).

CTHA

CTHA was performed using 16-row multi-slice CT machines from two manufacturers (Aquilion 16; Toshiba Medical Systems, Otawara, Tochigi, Japan and Sensation 16; Siemens Healthcare, Erlangen, Germany) after an angiographic catheter was positioned in the common hepatic artery or replaced right/left hepatic artery. First, CTHA including the whole liver was performed 5 s after starting injection of the contrast medium (1 mL/s; total dose, 30 mL), followed by a second-phase scan 30 s after the first scan. The dyn-CTHA scan location was based on the CTHA findings. After an interval of more than 5 min, dyn-CTHA scanning began immediately before injection of the contrast medium (1 mL/s; total dose, 10 mL), and a maximal 60-s continuous scan was obtained

in a single breath-hold with inhalation of oxygen (2 mL/s) (Fig. 2). The parameters of each CT scan were as follows: tube voltage, 130 and 120 kV; tube current, 150 and 200 mA; rotation time, 1.0 and 0.5 s; and collimation, 3.6 and 3.0 mm, respectively. Dyn-CTHA was performed in 12 patients by one CT unit using the former parameters and in 2 patients by the other CT unit using the latter parameters. Other parameters were as follows: field of view, 272–360 mm × 272–360 mm and matrix, 512 × 512. Images of four consecutive slices were reconstructed at 1-s intervals; i.e., temporal resolution of the CT images was 1 s. All dyn-CTHA examinations were performed within 3 weeks before or after DCE-MRI.

Image analysis

Only the arterial phases of DCE-MRI and dyn-CTHA were independently reviewed by two radiologists with 22 and 18 years of abdominal imaging experience, respectively, who were blinded to the patients' clinical backgrounds and pathological findings, except for the diagnosis of HCC. Disagreement was resolved by discussion and consensus. Tumor-enhancing findings such as early staining, peri-tumoral signal/attenuation,

corona enhancement, and washout were analyzed on both DCE-MRI and dyn-CTHA.

A detailed description of each finding is presented below.

・*Early staining* Stronger enhancement of the tumor than of the adjacent liver parenchyma on the arterial phase of DCE-MRI or dyn-CTHA soon after injection of the contrast agent (Figs. 3, 4).

・*Peri-tumoral low-intensity or low-density band* Low-signal or low-density band observed around the enhancing tumor (Figs. 3, 4).

・*Corona enhancement* Enhancement projected into the surrounding liver after enhancement of the whole tumor [4] (Fig. 3).

・*Washout* Intra-tumoral low-intensity area (at late arterial phase of DCE-MRI) or low-density area (in any phase of dyn-CTHA) compared with adjacent liver parenchyma after early staining (Figs. 4, 5).

The time point at which washout appeared was analyzed on dyn-CTHA, and the tumor enhancement time (defined as the duration for which the tumor was seen as a high-density/-intensity area compared with adjacent liver parenchyma, was assessed on both DCE-MRI and dyn-CTHA. If tumor enhancement was seen on one series of

sub-frame images on DCE-MRI, the tumor enhancement time was considered to be 3 s. If enhancement was seen on two series of sub-frame images, it was considered to be 6 s. On dyn-CTHA, the tumor enhancement time was considered to be the number of image series on which tumor enhancement was seen.

Statistical analysis

Inter-reader agreement was assessed by calculating the kappa statistic. A kappa value of ≤0.20 indicated poor agreement, 0.21 to 0.40 indicated fair agreement, 0.41 to 0.60 indicated moderate agreement, 0.61 to 0.80 indicated good agreement, and 0.81 to 1.00 indicated excellent agreement. The correlation of and difference in the tumor enhancement time between DCE-MRI and dyn-CTHA were analyzed using Spearman's rank correlation coefficient and Wilcoxon's signed rank test, respectively. A P value of <0.05 was considered to indicate a statistically significant difference. Statistical analyses were performed with a commercial software package (Prism, ver. 7; GraphPad Software, La Jolla, CA, USA) and Microsoft Excel 2016 (Microsoft, Redmond, WA, USA).

Results

A summary of the findings in each patient is shown in Table 2. Four findings were observed with both diagnostic imaging techniques: early staining, peri-tumoral low-intensity or low-density bands, corona enhancement, and washout of HCC. In all patients, early staining was seen at the arterial phase of DCE-MRI and dyn-CTHA. On DCE-MRI, all cases of early staining, low-intensity or low-density bands around the tumor, and corona enhancement were observed at the arterial phase (Fig. 3). All cases of corona enhancement were seen on the arterial phase of DCE-MRI, especially in the seventh or eighth sub-frame (late arterial phase) (Fig. 3). Partial washout was seen on the seventh or eighth sub-frame images of the arterial phase of DCE-MRI in four patients and on dyn-CTHA in all patients; the median washout appearance time was 25 s (range, 12–45 s) after the beginning of early staining (Fig. 4). Whole washout was seen at the portal venous phase of DCE-MRI in 11 patients and in the second phase of CTHA in all patients; it was not seen on DCE-MRI in 2 patients (Fig. 5).

Pathologically, a fibrous capsule was observed in 8 of 14 HCCs. It was seen in 7 of

10 HCCs with peri-tumoral low intensity on DCE-MRI and seen in 7 of 12 HCCs with peri-tumoral low density on dyn-CTHA.

The findings of early staining on DCE-MRI/dyn-CTHA, corona enhancement on dyn-CTHA, and washout on dyn-CTHA were fully matched between the two readers as positive findings. The kappa values of peri-tumoral low-signal/low-density bands on DCE-MRI/dyn-CTHA, corona enhancement on DCE-MRI, and washout on DCE-MRI were 0.8108/0.6316, 0.7586, and 0.6889, respectively. There were no findings of poor, fair or moderate inter-reader agreement.

The median tumor enhancement time on r-VIBE-KWIC and dyn-CTHA was 24 s (range, 9–24 s) and 23 s (range, 8–35s), respectively. The correlation coefficient of the tumor enhancement time between the two diagnostic imaging techniques was 0.762 ($P = 0.002$). There was no statistically significant difference between the two methods ($P = 0.2981$).

Discussion

On MRI, balancing the competing goals of image quality and high temporal resolution

is challenging because a trade-off between image quality and acquisition time becomes unavoidable. Various MR sequences with high temporal resolution have been reported and the feasibility of DCE-MRI for liver evaluation has been analyzed [9-12]. However, these techniques degrade the image quality or temporal fidelity. Some previous studies have been performed using nonspecific extracellular contrast agents, which have an advantage over Gd-EOB-DTPA with respect to arterial enhancement [13-15]. In addition, some problems have been reported in the arterial phase of DCE-MRI using Gd-EOB-DTPA, such as suboptimal timing and transient severe motion [8, 16, 17]. The r-VIBE-KWIC sequence is one candidate for overcoming these problems because it has motion resistance and provides images with high temporal resolution without degradation of the image quality in the arterial phase of DCE-MRI [8].

With respect to the assessment of the detailed arterial hemodynamics of HCC, CTHA (especially dyn-CTHA) has been considered the gold standard for the evaluation of early staining, corona enhancement, and washout. To the best of our knowledge, no studies have compared the findings of DCE-MRI and dyn-CTHA. Because dyn-CTHA is a relatively invasive technique with the added drawback of radiation exposure and its

scan coverage is more limited than that of DCE-MRI, it is very useful to obtain dyn-CTHA-like images by DCE-MRI for accurate diagnosis.

In the present study, all hypervascular HCCs were accurately demonstrated on DCE-MRI. This suggests that the optimal timing of the arterial phase and adequate arterial enhancement were obtained in DCE-MRI using r-VIBE-KWIC. These phenomena were validated by Fujinaga et al. [8].

Peri-tumoral low-intensity or low-density bands, which have not been previously reported, were seen on DCE-MRI in 83% of HCCs. Initially, we suspected that this finding corresponded to the pseudocapsule of HCC. However, of 12 HCCs with a low-density band around the tumor on dyn-CTHA, 4 had no pseudocapsule on pathological examination. Because a detailed correlation between the radiologic and pathologic findings was not performed in this study, the significance of this finding remains uncertain.

Corona enhancement, which is always observed in HCCs on dyn-CTHA [4], was evaluated on DCE-MRI in 78% of HCCs in this study. It appeared as a transient corona or wedged-shaped enhancement just after tumor enhancement, and the shape of the

enhancement on DCE-MRI and dyn-CTHA was the same in each patient. Ueda et al. [4] reported that contrast enhancement of the adjacent liver and corona enhancement began 10.5 ± 2.2 and 22.4 ± 6.1 s after the start of the injection, respectively. High temporal resolution of the images was needed to demonstrate this finding. In the present study, detailed serial arterial hemodynamic changes of HCC were clearly evaluated on DCE-MRI using r-VIBE-KWIC. However, corona enhancement was not observed in three patients. We speculate that there are two reasons for this phenomenon. One might be the failure to obtain optimal arterial phase images because of shorter scan time of DCE-MRI (24 s) than dynamic CTHA (60 s). Another factor might be the increased signal intensity in the adjacent region because of the portal venous flow on the DCE-MRI.

Partial washout was seen only in 29% of HCCs on the arterial phase of DCE-MRI, although it was seen in all HCCs on dyn-CTHA. We attribute this phenomenon to differences in the acquisition and scan times; i.e., the acquisition time of DCE-MRI was shorter than the scan time of dyn-CTHA. In other words, this result indicates that early staining would be underestimated in the arterial phase of DCE-MRI when the

acquisition time is long. This occurs because washout of HCC begins in the arterial phase of DCE-MRI, and the coexistence of early staining (high signal intensity) and washout (low signal intensity) in the arterial phase results an averaged signal between them.

In two HCCs, washout was not seen on DCE-MRI although it was seen on CTHA. In these patients, the HCC was shown as a hyperintense area compared with the adjacent liver (Fig. 5). This seems to be one of the pitfalls in assessing washout on DCE-MRI.

The concordance rate of each finding on both modalities was acceptable because some findings were fully matched between the two readers and others showed good or excellent inter-reader agreement.

Our study has some limitations. First, only a small number of patients who underwent hepatic resection were analyzed in this study. Second, the MRI scan parameters varied, and two different CT systems were used. A prospective study might be required to overcome this problem. Third, the maximum tumor enhancement time on DCE-MRI was limited to ≤24 s because the acquisition time of DCE-MRI was limited.

However, oxygen inhalation may allow for a longer breath-hold time comparable with dyn-CTHA.

In conclusion, DCE-MRI with high temporal resolution using r-VIBE-KWIC has diagnostic potential comparable with that of dyn-CTHA in the hemodynamic evaluation of HCC except for the washout phenomenon.

References

1. Hayashi M, Matsui O, Ueda K, Kawamori Y, Kadoya M, Yoshikawa J, et al. Correlation between the blood supply and grade of malignancy of hepatocellular nodules associated with liver cirrhosis: evaluation by CT during intraarterial injection of contrast medium. AJR Am J Roentgenol. 1999;172(4):969-76.

2. Matsui O, Kadoya M, Kameyama T, Yoshikawa J, Takashima T, Nakanuma Y, et al. Benign and malignant nodules in cirrhotic livers: distinction based on blood supply. Radiology. 1991;178(2):493-7.

3. Hayashi M, Matsui O, Ueda K, Kawamori Y, Gabata T, Kadoya M. Progression to hypervascular hepatocellular carcinoma: correlation with intranodular

blood supply evaluated with CT during intraarterial injection of contrast material. Radiology. 2002;225(1):143-9.

4. Ueda K, Matsui O, Kawamori Y, Nakanuma Y, Kadoya M, Yoshikawa J, et al. Hypervascular hepatocellular carcinoma: evaluation of hemodynamics with dynamic CT during hepatic arteriography. Radiology. 1998;206(1):161-6.

5. Kitao A, Zen Y, Matsui O, Gabata T, Nakanuma Y. Hepatocarcinogenesis: multistep changes of drainage vessels at CT during arterial portography and hepatic arteriography--radiologic-pathologic correlation. Radiology. 2009;252(2):605-14.

6. Vigen KK, Peters DC, Grist TM, Block WF, Mistretta CA. Undersampled projection-reconstruction imaging for time-resolved contrast-enhanced imaging. Magn Reson Med. 2000;43(2):170-6.

7. Song HK, Dougherty L. Dynamic MRI with projection reconstruction and KWIC processing for simultaneous high spatial and temporal resolution. Magn Reson Med. 2004;52(4):815-24.

8. Fujinaga Y, Ohya A, Tokoro H, Yamada A, Ueda K, Ueda H, et al. Radial volumetric imaging breath-hold examination (VIBE) with k-space weighted image

contrast (KWIC) for dynamic gadoxetic acid (Gd-EOB-DTPA)-enhanced MRI of the liver: advantages over Cartesian VIBE in the arterial phase. Eur Radiol. 2014;24(6):1290-9.

9. Mori K, Yoshioka H, Takahashi N, Yamaguchi M, Ueno T, Yamaki T, et al. Triple arterial phase dynamic MRI with sensitivity encoding for hypervascular hepatocellular carcinoma: comparison of the diagnostic accuracy among the early, middle, late, and whole triple arterial phase imaging. AJR Am J Roentgenol. 2005;184(1):63-9.

10. Yoshioka H, Takahashi N, Yamaguchi M, Lou D, Saida Y, Itai Y. Double arterial phase dynamic MRI with sensitivity encoding (SENSE) for hypervascular hepatocellular carcinomas. J Magn Reson Imaging. 2002;16(3):259-66.

11. Hong HS, Kim HS, Kim MJ, De Becker J, Mitchell DG, Kanematsu M. Single breath-hold multiarterial dynamic MRI of the liver at 3T using a 3D fat-suppressed keyhole technique. J Magn Reson Imaging. 2008;28(2):396-402.

12. Kanematsu M, Goshima S, Kondo H, Yokoyama R, Kajita K, Hoshi H, et al. Double hepatic arterial phase MRI of the liver with switching of reversed centric and

centric K-space reordering. AJR Am J Roentgenol. 2006;187(2):464-72.

13. Tamada T, Ito K, Sone T, Yamamoto A, Yoshida K, Kakuba K, et al. Dynamic contrast-enhanced magnetic resonance imaging of abdominal solid organ and major vessel: comparison of enhancement effect between Gd-EOB-DTPA and Gd-DTPA. J Magn Reson Imaging. 2009;29(3):636-40.

14. Kuhn JP, Hegenscheid K, Siegmund W, Froehlich CP, Hosten N, Puls R. Normal dynamic MRI enhancement patterns of the upper abdominal organs: gadoxetic acid compared with gadobutrol. AJR Am J Roentgenol. 2009;193(5):1318-23.

15. Fujinaga Y, Ueda H, Kitou Y, Tsukahara Y, Sugiyama Y, Kadoya M. Time-intensity curve in the abdominal aorta on dynamic contrast-enhanced MRI with high temporal and spatial resolution: Gd-EOB-DTPA versus Gd-DTPA in vivo. Japanese journal of radiology. 2012.

16. Davenport MS, Viglianti BL, Al-Hawary MM, Caoili EM, Kaza RK, Liu PS, et al. Comparison of acute transient dyspnea after intravenous administration of gadoxetate disodium and gadobenate dimeglumine: effect on arterial phase image quality. Radiology. 2013;266(2):452-61.

17. Pietryga JA, Burke LM, Marin D, Jaffe TA, Bashir MR. Respiratory motion artifact affecting hepatic arterial phase imaging with gadoxetate disodium: examination recovery with a multiple arterial phase acquisition. Radiology. 2014;271(2):426-34.

Figures and Figure Legends

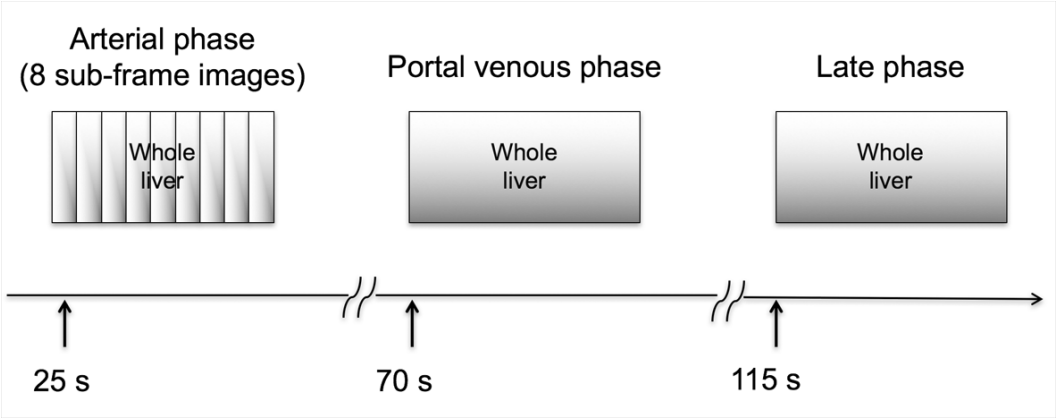

Fig. 1 Protocol of dynamic contrast-enhanced magnetic resonance imaging

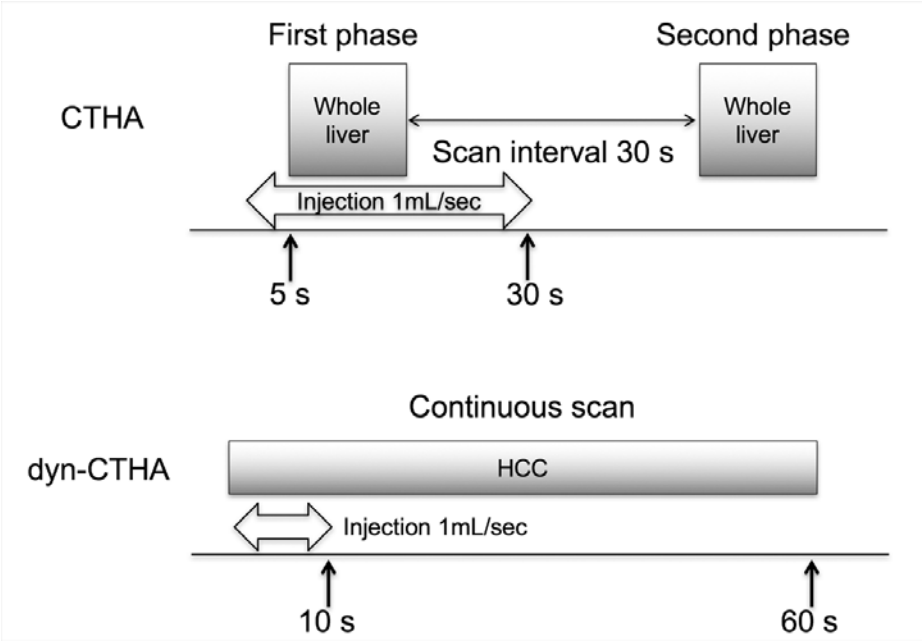

Fig. 2 Protocol of CTHA and dyn-CTHA

CTHA: computed tomography during hepatic arteriography; dyn-CTHA: dynamic

CTHA

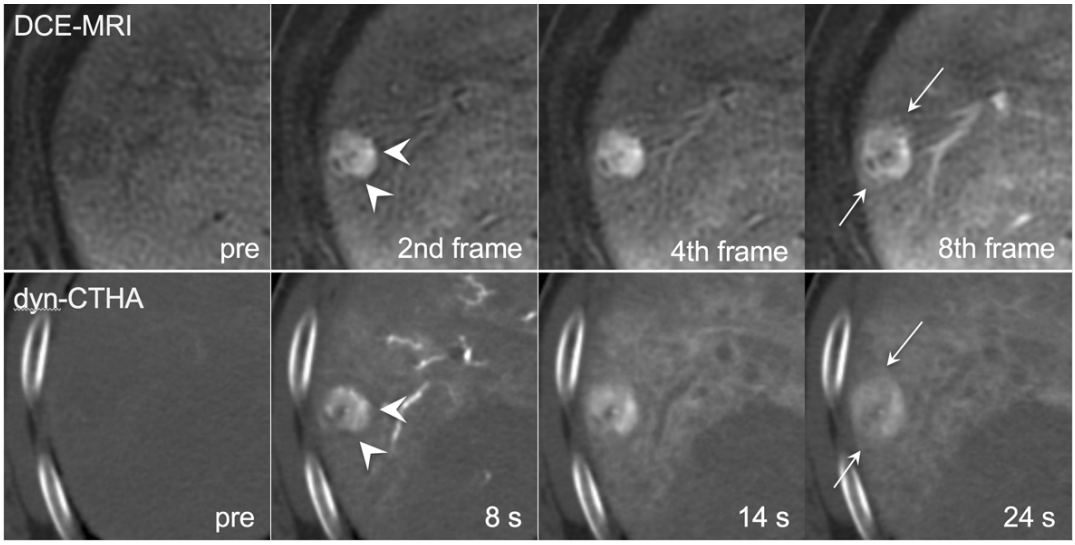

Fig. 3 A 66-year-old man with hepatocellular carcinoma

Early staining, a peri-tumoral low-intensity/-density band (white arrowheads), and corona enhancement (thin arrows) are seen on the arterial phase of DCE-MRI (upper row) and dyn-CTHA (lower row). DCE-MRI: dynamic contrast-enhanced magnetic resonance imaging; dyn-CTHA: dynamic computed tomography during hepatic arteriography

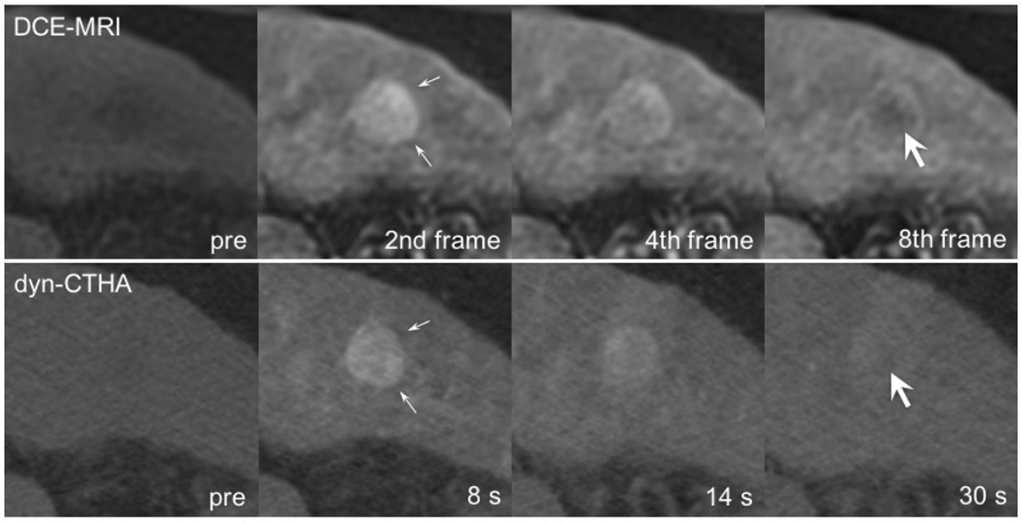

Fig. 4 A 66-year-old woman with hepatocellular carcinoma

Early staining, peri-tumoral low-intensity/-density band, (small white arrows), and partial washout (white arrows) are seen on the arterial phase of DCE-MRI (upper row) and dyn-CTHA (lower row). DCE-MRI: dynamic contrast-enhanced magnetic resonance imaging; dyn-CTHA: dynamic computed tomography during hepatic arteriography

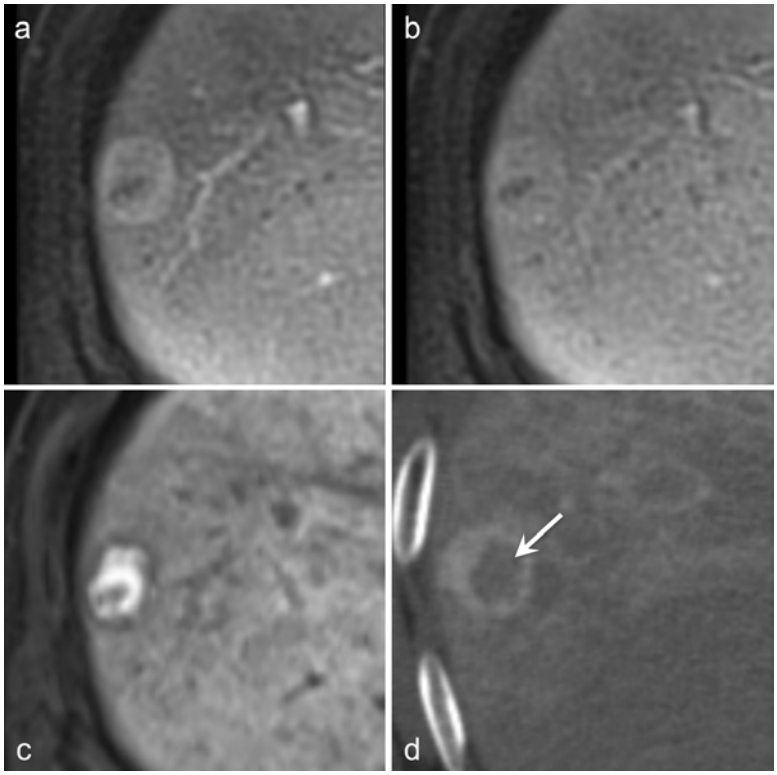

Fig. 5 A 66-year-old man with hepatocellular carcinoma (same patient as in Figure 3) Washout is not seen on the portal venous or late phases of DCE-MRI (a, b). At the hepatobiliary phase (c), the tumor is shown as a hyperintense area compared with the adjacent liver. On the second phase of CTHA (d), washout is seen (white arrow).

Tables and Table Legends

Table 1 Scan parameters of dynamic contrast-enhanced magnetic resonance imaging using radial volumetric imaging breath-hold examination with k-space-weighted image contrast reconstruction

Repetition time (ms)	2.55–3.20
Echo time (ms)	1.11–1.21
Flip angle (degrees)	12–13
Matrix size	160–256 × 160–256
Section thickness (mm)	4.0–4.2
Field of view (mm)	280–480 × 280–480
Acquisition time (s)	21–24
Parallel imaging	No
Number of time-resolved images	8

Table 2 Summary of DCE-MRI and dyn-CTHA findings

HCC findings on DCE-MRI and dyn-CTHA	DCE-MRI (n = 14)	dyn-CTHA (n = 14)	DCE-MRI /dyn-CTHA (%)
Early staining	14	14	100
Low-signal/-density band around the tumor	10	12	83
Corona enhancement	11	14	78
Partial washout	4	14	29

DCE-MRI, dynamic contrast-enhanced magnetic resonance imaging; dyn-CTHA, dynamic computed tomography during hepatic arteriography; HCC, hepatocellular carcinoma